



An *In Vivo* Molecular Imaging Technique Broadly Applicable For Determining Antitumor Efficacy And/Or Collateral Tissue Damage By Oncologic Drugs And Therapies With Cytotoxic Effects

Rationale: In oncological drug R&D, efficacy and safety are important considerations in identifying pharmaceutical candidates for prioritization and eventual marketing. Successful anticancer therapies are as much about killing malignancies as preserving normal tissues. While cancer cells are the primary target for therapeutic agents, side effects are also critical attributes of a drug candidate. In the current document, we present an *in vivo* imaging tool for characterizing chemotherapeutic agents/treatments in preclinical settings with spatiotemporal measurements simultaneously on the efficacy of tumor kill and systemic tissue damage induced by cytotoxic side effects. The data also allow semi-quantitative comparison among drug candidates or different treatments (between monotherapies as well as mono- vs. combination therapies). The outcome of these studies enables expedited decision making for determining efficacious and safe candidates for prioritization while eliminating those with poor performance and excessive toxicity.

Our technology: This *in vivo* imaging technology is dedicated to and optimized for assessing tissue injury systemically, including tumor and nontumor tissues. The technology detects molecular signatures of cell death, including apoptosis, as an important manifestation of terminal cellular response to cytotoxic stimuli. Compared to other molecular and biochemical assays which detect metabolic and signaling changes, cell death is an unambiguous marker for cytotoxicity. Our imaging technique targets phosphatidylethanolamine (PE) for its capacity in detecting cell death as a surrogate marker for tissue damage. PE is a type of aminophospholipid which is sequestered inside normal cells but is externalized and becomes accessible when a cell is dead or dying. This near-universal marker, which relies on phospholipid redistribution, allows for the detection of multiple forms of cell death regardless of causes or pathways. This is particularly important because there is extensive signaling cross talk among mechanisms of cell death in which different cell/tissue types respond differently to cytotoxic stimuli, and wherein the propensity toward one mode of cell death over another may differ. Such an imaging technique is therefore of practical advantage where tumor kill and off-target tissue damage can be assessed simultaneously and systemically as opposed to a particular pathway or mode of cell death. This approach is applicable without prior knowledge of drug effects, thus serving as a useful survey for tissue susceptibility in response to drug toxicity.

Areas of applications: Our technology detects a near universal molecular marker for cell death; it is thus potentially applicable for a broad range of therapeutic and pathological changes as a result of tissue damage from cytotoxic drugs and treatments. Valuable data can be derived from specific tissues/organs or in a whole-body fashion. Applications include but are not limited to the following:

- Assessment of organ-specific tissue damage, such as drug-induced liver injury (DILI), renal toxicity, myelosuppression, cardiotoxicity, etc.
- Whole-body survey for tissue/organ susceptibility to cytotoxicity without prior knowledge.
- Determination of antitumor efficacy and prioritization of drug candidates.
- Simultaneous measurements of antitumor efficacy and cytotoxicity-induced off-target damage.
- Optimizing drug dosing/regimens for maximized efficacy and minimal off-target damage.

- Characterizing the therapeutic efficacy and adverse side effects of oncologic treatments, including chemotherapies, radiation therapies, immunotherapies (CAR T, antibodies, immunomodulators), viral therapies.
- Preemptive assessment on drug safety for minimizing black box warning risk.
- Providing comparative data among drugs/treatments (prioritization among drug candidates, comparing mono- versus combination therapies, etc.)

Other benefits of the technology include:

- The technology is aligned with the principles of the 3Rs (Replacement, Reduction and Refinement).
- By being minimally invasive, the technology enables continuous studies in the same animals over time with repeated measurements. As such, the technology is compatible with both acute and longitudinal studies. After the completion of the imaging study, the animals can be transported back to the customer for further evaluations as needed.
- With data obtained using this technology, the information can help reduce the attrition rate by determining potential safety issues early.
- The technology can help identify efficacious and safe drug candidates for prioritization while eliminating ineffective and/or overly toxic candidates in a more streamlined R&D process. A drawing which shows the general workflow of this technology is illustrated in Figure 1.

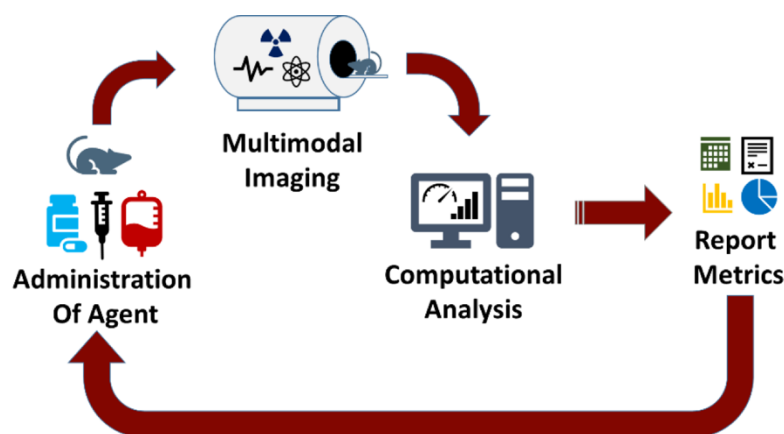


Figure 1. An overview of the workflow of this technology. *In vivo* imaging data are acquired on preclinical animal models treated with drugs or therapies, where the data provide indicators for tumor kill (antitumor efficacy) and/or systemic susceptibility (toxicity-induced damage in off-target tissues). The technology can be deployed for single drug assessments, comparison among multiple drug candidates, or mono- versus combination therapies. The data allow semi-quantitative assessments of drugs and therapies. This technology can be applied iteratively along multiple stages along the drug R&D process for identifying safe and efficacious candidates while help eliminating ineffective and/or overly toxic compounds.

Demonstrations of utilities:

Showcase I: Assessing tissue damage induced by cytotoxic drugs. A single dose of cisplatin (CDDP) was administered at 2 mg/kg intraperitoneally in Sprague Dawley rats. *In vivo* imaging data were acquired on day-5 post treatment. Wide spread tissue damages were identified by *in vivo* imaging (Figure 2) and validated by histopathology.

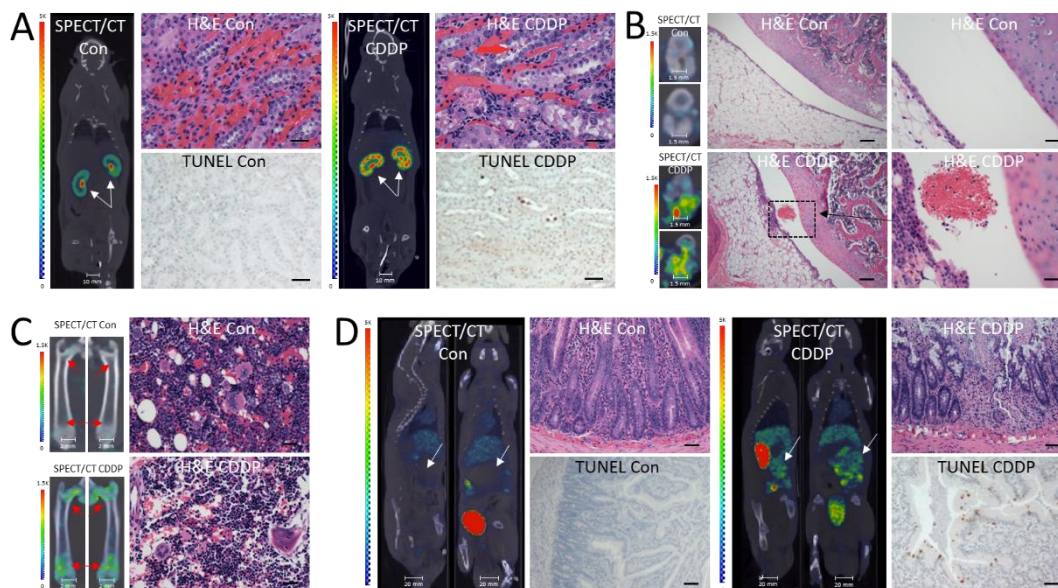


Figure 2. Assessment of cisplatin-induced tissue damage. A) Cisplatin (CDDP) treatment caused significant signal elevation in renal cortex as validated by corresponding histopathology (TUNEL staining for apoptotic nuclei). B) Knee joint damage was identified by *in vivo* imaging as focal signals, which was confirmed by histopathology with injury to the joint lining and the presence of thrombus. C) Images of the femurs in control and treated animals are presented. Significant signal elevation was detected in the symphysis of the bones. H&E stained section of femoral bone demonstrates a depletion of hematopoietic cells in bone marrow of treated animals. D) Damages to the guts were identified with *in vivo* imaging as seen in corresponding TUNEL micrographs (apoptotic nuclei were stained positive with the deposition of brown pigment).

Showcase II: Dynamic systemic tissue susceptibility to cytotoxic drugs. Dynamic *in vivo* imaging data were acquired in cyclophosphamide-treated Sprague Dawley rats (80 mg/kg) at baseline and days 1, 3, 5 and 7 post treatment. The dynamics of signal changes is shown in Figure 3.

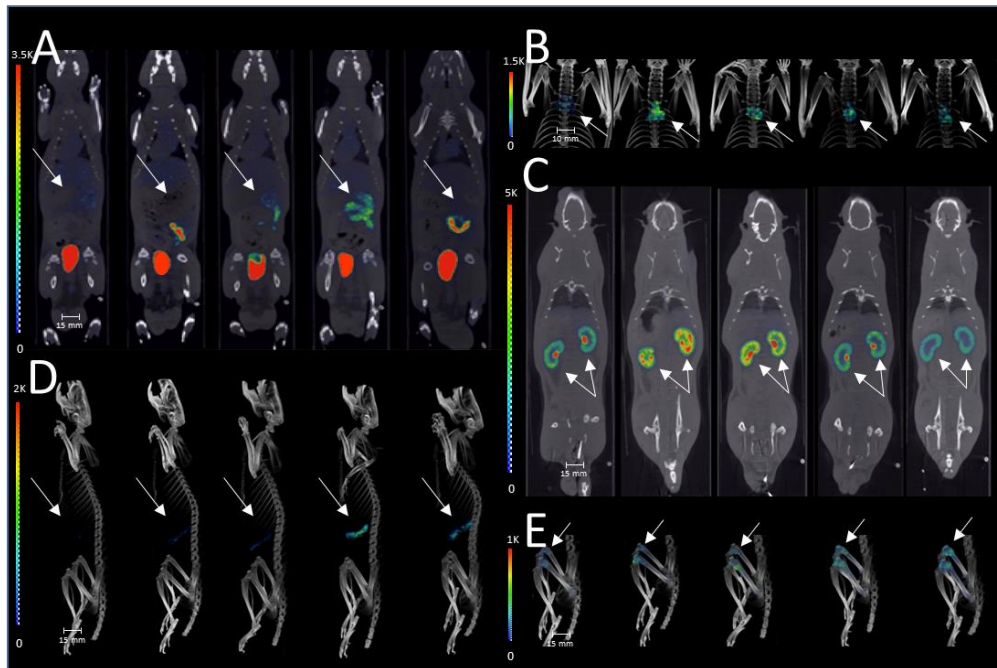


Figure 3. Dynamic imaging of cyclophosphamide treated rats. Signal changes in each tissue at before drug administration, days 1, 3, 5 and 7 post cyclophosphamide treatment are shown in the gut (A), thymus (B), kidneys (C), spleen (D) and femurs/knees (E) over the course of 7 days after treatment. Note that the onset and progression of tissue injury differ in a spatiotemporal fashion.

Showcase III: Tissue susceptibility to cytotoxic drugs in an individualized basis. *In vivo* data were acquired in cyclophosphamide-treated Sprague Dawley rats, identifying changes in signal intensity in a wide range of tissues and organs. The data also demonstrated personalized response to a given drug treatment, as shown in Figure 4.

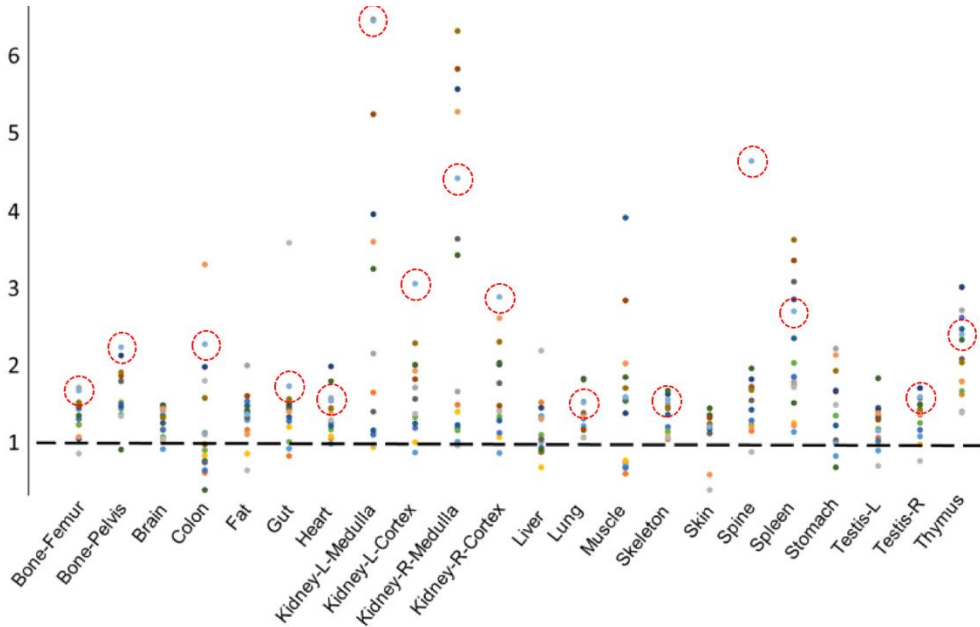


Figure 4. *In vivo* data in rats at 2 days after cyclophosphamide treatment (80 mg/kg). The ratios of signal changes to control in each tissue are shown. Note that a ratio greater than 1 indicates elevated signal change compared to control. Also note each individual animal is color-coded, so that the systemic changes can be examined in a personalized fashion. An example of an individual which was highly responsive to the drug treatment across many tissue and organs is highlighted in red circles.

Showcase IV: Gender-based dynamic systemic tissue susceptibility to cytotoxic drugs. Dynamic *in vivo* imaging data were acquired in cyclophosphamide-treated male and female Sprague Dawley rats (80 mg/kg) at baseline and days 1, 3, 5 and 7 post treatment. The signal changes were compared between the two sexes.

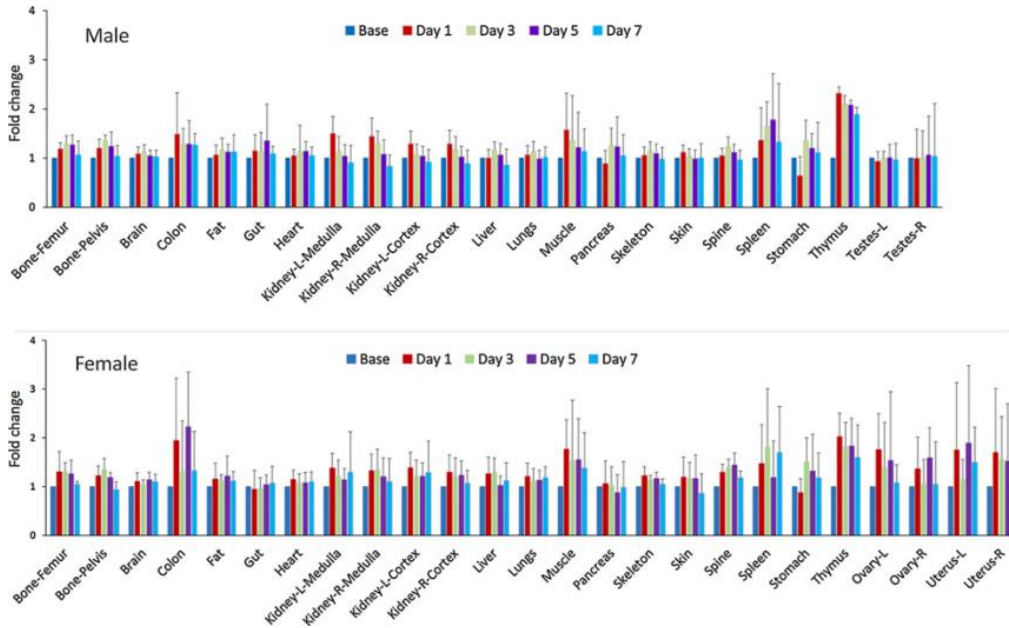


Figure 5. Signal changes in a gender-based study. Signal changes in each tissue at before drug administration, days 1, 3, 5 and 7 post cyclophosphamide treatment are shown in male versus female rats. Note these whole-body dynamic data sets also contain individualized data for personalized analyses in scatter plots as illustrated in Figure 4.

Showcase V: Simultaneous assessment of antitumor efficacy and systemic tissue damage. In this study our technology demonstrated values in: 1) determining the antitumor efficacy and systemic adverse effects by chemotherapeutic drugs; 2) comparing the efficacy and toxicity between individual drugs; and 3) assessing the outcome of a combination therapy of the two drugs by identifying that drug B was the dominant drug in the combination therapy and that the combination therapy did not significantly improve antitumor efficacy while resulted in greater systemic toxicity. Multiple myeloma tumor-bearing mice were treated with either drug A, or drug B or a combination of the two, and *in vivo* imaging data were acquired at baseline and on days 1, 3 and 5 post treatment. Data on antitumor efficacy are shown as indicated by the spatial temporal changes in tumor signal intensity (Figures 6 and 7) which were validated by histopathology (Figure 8).

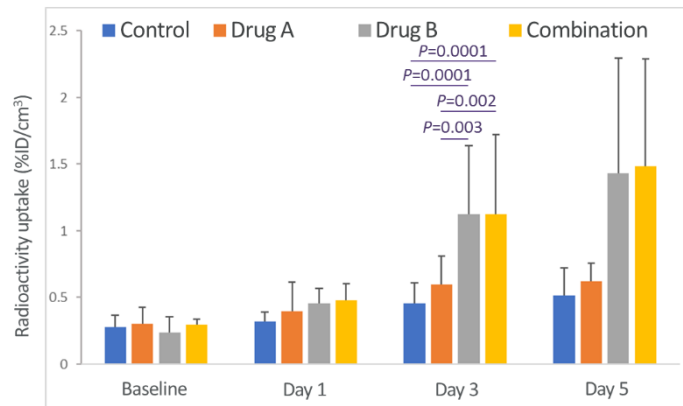


Figure 6. *In vivo* signal changes in the tumor among control (n=8), drug A (n=8), drug B (n=8) and combination therapy (n=9) groups before (baseline) and at days 1, 3 and 5 after treatment.

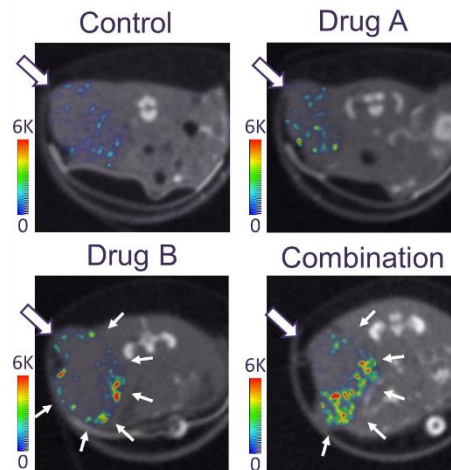


Figure 7. The pattern of signal distribution in the tumor was different as a result of different treatments. While there was diffusive signal throughout the tumor tissue with drug A, more intense signal was distributed to the periphery of the tumor with drug B and combination therapy. The tumor was indicated with a block arrow; tumor periphery was marked with arrowheads.

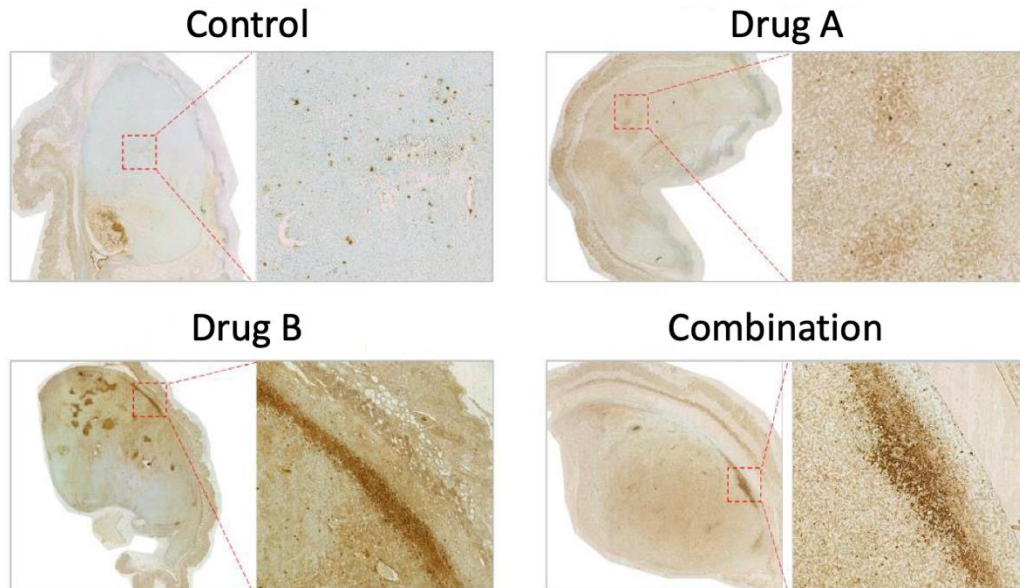


Figure 8. TUNEL staining of excised tumor tissues on day-5, indicating diffused distribution of apoptotic nuclei throughout the tumor tissue in control and drug A groups. In contrast, high density of apoptotic nuclei was identified in the tumor periphery after drug B and combination therapy treatment. The findings were consistent with *in vivo* imaging data (Figure 7).